NINTH EUROPEAN ROTORCRAFT FORUM

Paper No. 56

HELICOPTER INDIVIDUAL-BLADE-CONTROL AND ITS APPLICATIONS

N.D. Ham

Department of Aeronautics and Astronautics
Massachusetts Institute of Technology
Cambridge, Massachusetts
U.S.A.

September 13-15, 1983

STRESA, ITALY

Associazione Industrie Aerospaziali

Associazione Italiana di Aeronautica ed Astronautica

HELICOPTER INDIVIDUAL-BLADE-CONTROL AND ITS APPLICATIONS

Norman D. Ham

Director, VTOL Technology Laboratory
Department of Aeronautics and Astronautics
Massachusetts Institute of Technology
Cambridge, Massachusetts 02139

Abstract

A new, advanced type of active control for helicopters and its applications are described.

The system, based on previously developed M.I.T. Individual-Blade-Control hardware, employs blade-mounted accelerometers to sense blade motion and feeds back information to control blade pitch in such a manner as to reduce the response of selected blade modes. A linear model of the blade and control system dynamics is used to give guidance in the design process as well as to aid in analysis of experimental results. System performance in wind tunnel tests is described, and evidence is given of the system's ability to provide substantial reduction in blade modal responses, including blade bending vibration.

Introduction

A truly advanced helicopter rotor must operate in a severe aerodynamic environment with high reliability and low maintenance requirements. This environment includes:

(1) atmospheric turbulence (leading to impaired flying qualities, particularly in the case of hingeless rotor helicopters).

(2) retreating blade stall (leading to large torsional loads in blade structure and control system).

(3) blade-vortex interaction in transitional and nap-of-the-earth flight (leading to unacceptable higher harmonic blade bending stresses and helicopter vibration).

(4) blade-fuselage interference (leading to unacceptable higher harmonic blade bending stresses and helicopter vibration).

(5) blade instabilities due to flap-lag coupling and high advance ratio (including blade "sailing" during shut-down).

The application of feedback techniques make it possible to alleviate the effects described in items (1) to (5) above, while improving helicopter vibration and handling characteristics to meet desired standards. The concept of Individual-Blade-Control (IBC) embodies the control of broad-band electrohydraulic actuators attached to each blade, using signals from sensors mounted on the blades to supply appropriate control commands to the actuators[1-6]. Note that the IBC involves not just control of each blade independently, but also a feedback loop for each blade in the rotating frame. In this manner it becomes possible to reduce the severe effects of atmospheric turbulence, retreating blade stall, blade-vortex interaction, blade-fuselage interference, and blade instabilities, while providing improved flying qualities and automatic blade tracking.

It is evident that the IBC system will be most effective if it is comprised of several sub-systems, each controlling a specific mode, e.g., the blade flapping mode, the first blade lag mode, the first blade flatwise bending mode, and the first blade torsion mode. Each sub-system operates in its appropriate frequency band.

The configuration used in this investigation employs an individual actuator and multiple feedback loops to control each blade. These actuators and feedback loops rotate with the blades and, therefore, a conventional swash plate is not required. However, the same degree of individual blade-control can be achieved by placing the actuators in the non-rotating system and controlling the blades through a conventional swash plate if the number of control degrees-of-freedom equals the number of blades. For more than three blades, the use of extensible blade pitch control rods in the form of hydraulic actuators is a possibility. See Ref. 6 for some other design solutions.

The present paper is primarily concerned with the application of the Individual-Blade-Control concept to vertical alleviation. Other applications are described in the Appendix.

Helicopter higher harmonic vertical hub shears and the resulting vibration are due to

This research was sponsored by the Ames Research Center, NASA, Moffett Field, California 94035.

three major sources[7]: higher harmonic blade residual lift (the aerodynamic forcing function less aerodynamic forces due to blade flapping), the inertial loading due to higher harmonic blade flapping response, and the inertial loading due to higher harmonic blade first elastic mode flatwise bending response. These sources are shown in rotating vector (phasor) form in Fig. 1, from Ref. 8, for the case of third harmonic vertical hub shear. The hub shear components due to blade residual lift and flapping inertial reaction tend to cancel each other; the hub shear component due to blade first elastic mode bending inertial reaction is the major source of vibration.

The near cancellation of blade lift and flapping inertial shears is due to the fact that the higher harmonic aerodynamic forcing frequencies ($\geq$2P) are far above the blade flapping natural frequency near 1P. Then the blade flapping inertial response lags the aerodynamic input by nearly 180 degrees and cancellation occurs. For further discussion, see Ref. 8.

Thus a major source of vertical vibration is the blade first elastic mode bending response to higher harmonic airloads: if the blade bending response is reduced, the vertical vibration will be correspondingly reduced.

Another source of high-frequency blade bending vibration is blade-fuselage interference. Figure 2, from Ref. 9, shows the incremental flatwise bending moment on a model helicopter blade due to the presence of the fuselage. Note that the time history is essentially that of the lightly damped first elastic bending mode of the blade responding at its natural frequency of about 5P to an impulsive disturbance: the maximum upwash at the rotor plane due to the fuselage occurs approximately over the nose of the fuselage and is impulsive in nature.

Since the major source of blade incremental flatwise bending moment is the response of the blade first elastic bending mode, if the blade bending response is reduced, the effect of blade-fuselage interference on vertical vibration will be correspondingly reduced.

This paper is primarily concerned with the application of the IBC concept to control of the blade first elastic flatwise bending mode. To achieve this, a servomotor controls the pitch angle of the blade whose flatwise acceleration and displacement are sensed by three accelerometers, and an integrator yields the flatwise velocity. Combinations of these signals are fed back to the blade pitch control to effect increases in the effective inertia, damping, and stiffness of the blade first elastic flatwise bending mode.

Other applications are described in the Appendix.

Technical Discussion

Consider the dynamic system described by the differential equation

$$m\ddot{x} + c\dot{x} + kx = F \qquad (1)$$

For the case of forced vibration at frequency ω, $F = F_o \sin\omega t$, and equation (1) can be written

$$\ddot{x}/\omega_n^2 + (2\zeta/\omega_n)\dot{x} + x = (F_o/m\omega_n^2)\sin\omega t \qquad (2)$$

where

$\omega_n = (k/m)^{1/2}$, the system natural frequency

$\zeta = c/2m\omega_n$, the system damping ratio

$F_o/m\omega_n^2 = x_s$, the system static displacement

The solution of equation (2) is

$$\frac{x}{F_o/m\omega_n^2} = \frac{1}{\left\{\left[1-(\omega/\omega_n)^2\right]^2 + \left[2\zeta(\omega/\omega_n)\right]^2\right\}^{1/2}} \qquad (3)$$

For the case of an impulse I applied at $t = 0$, $F = I$, and equation (1) can be written

$$\ddot{x}/\omega_n^2 + (2\zeta/\omega_n)\dot{x} + x = I/m\omega_n^2$$

The solution of equation (3) is

$$\frac{x}{I/m\omega_n} = \frac{1}{\sqrt{1-\zeta^2}}\, e^{-\zeta\omega_n t} \sin\sqrt{1-\zeta^2}\ \omega_n t \qquad (4)$$

It is seen from equations (1) and (2) that if a means can be found to increase the effective value of the system parameter m to (1+K)m, while maintaining parameters ω_n and ζ constant, then the system response for sinusoidal and impulsive inputs will be reduced by the factor 1/(1+K).

Now equation (1) can be interpreted as the equation of motion of the kth blade flatwise bending mode due to either the nth harmonic airload or to the impulsive load due to blade/fuselage interference; if an incremental airload of magnitude $\Delta F = -K(m\ddot{x} + c\dot{x} + kx)$ is generated by control of individual blade pitch, then indeed the effective mass of the system will become (1+K)m while ω_n and ζ remain constant. Then the blade flatwise bending response and associated vertical inertial vibratory shear will be reduced by the alleviation factor 1/(1+K).

Note that there is diminishing effectiveness in blade bending alleviation by this method as

the gain K is increased: it appears that a response reduction of 75 to 80%, i.e. K = 3 to 4, is a practical goal.

The theory, design, and performance of a control system to achieve this goal is described in the following sections.

Theoretical Analysis

Following references 1 and 10, the kth blade flatwise bending equation of motion is given by

$$M_k \ddot{g}_k + M_k \omega_k^2 g_k = \int_0^R \eta_k \frac{dL}{dr} dr \qquad (5)$$

where $M_k = \int_0^R m\eta_k^2 dr$

$\eta_k(r)$ = kth flatwise bending mode shape

$g_k(t)$ = kth flatwise bending mode displacement

ω_k = kth flatwise bending mode natural frequency

R = rotor radius

Ω = rotor rotational speed

$\frac{dL}{dr}$ = blade flatwise aerodynamic loading per unit span

For present purposes only the first elastic flatwise bending mode will be considered. Then following Ref. 10 and writing $\eta_k = \eta$, $g_k = g$, $M_k = M$, and $\omega_k = \omega_g$, and neglecting time-dependent terms in the aerodynamic coefficients, equation (5) becomes

$$(M/I_1)\ddot{g} + m_{\dot{g}}\Omega \dot{g} + (M/I_1)\omega_g^2 g = m_\theta \Omega^2 \theta \qquad (6)$$

where $m_{\dot{g}} = \frac{\gamma}{2} \int_0^1 (\eta/R)^2 \, x dx$

$m_\theta = \frac{\gamma}{2} \int_0^1 (\eta/R) \, x^2 dx$

$x = r/R$

γ = blade Lock number

and $C'(k)$, the mean value of the lift deficiency function, is taken as unity for present purposes; any resulting error can be accommodated by increasing control system gain.

Then equation (6) gives the blade flatwise bending transfer function

$$\frac{g(s)}{\theta(s)} = \frac{m_\theta \Omega^2}{(M/I_1)s^2 + m_{\dot{g}} \Omega s + (M/I_1)\omega_g^2} \qquad (7)$$

Though this equation applies strictly to hover, it will be used as a first approximation for the case of forward flight in designing the control system.

Transfer functions for other blade bending modes can be obtained in a similar manner if required, e.g., the flapping mode β.

Bending Signal Extraction

Consider the blade shown in Figure 3 to be responding in both the flapping mode and the first elastic flatwise bending mode. The signal from an accelerometer placed at blade station x is given by

$$a_F/R\Omega^2 = x\ddot{\beta}/\Omega^2 + x\beta + \eta(x)\ddot{g}/\Omega^2 + x\eta'(x)g \qquad (8)$$

where R = rotor radius

Ω = rotor rotational speed

x = blade spanwise station r/R

$\beta(t)$ = blade flapping angle

$\eta(x)$ = first elastic flatwise bending mode shape

$g(t)$ = first elastic flatwise bending mode displacement

It is evident that if three flatwise-oriented accelerometers are mounted at three different spanwise stations, equation (8) yields three equations corresponding to the three spanwise stations. These equations can be solved for the three quantities $(\ddot{\beta}/\Omega^2 + \beta)$, $\ddot{g}/\Omega^2$, and g. Integration of $\ddot{g}/\Omega^2$ then yields bending rate $\dot{g}/\Omega$.

If $\ddot{\beta}/\Omega^2$ and β are required independently, then flapping hinge displacement $\beta + \eta'(0)g$ must be measured using an angular transducer to provide a fourth equation.

The above technique provides all the information required to create the bending feedback signals $(\ddot{g} + \omega_g^2 g)$, $\dot{g}$, and if desired, the flapping feedback signals $(\ddot{\beta} + \Omega^2\beta)$ and/or $\dot{\beta}$.

Control System Design

The design of the control system is based on the root locus of the overall system, composed of a servomotor controlling the pitch motion of the blade, which is equipped with three accelerometers to provide the required feedback signals as described in the previous section.

Equation (7) gives the blade bending transfer function.

The combined accelerometer transfer functions are given by

$$A_1(s) = \frac{R\Omega^2}{G}\left[\left(\frac{s}{\Omega}\right)^2 + \left(\frac{\omega_g}{\Omega}\right)^2\right]$$

and $$A_2(s) = \frac{R\Omega^2}{G}\left(\frac{s}{\Omega}\right)^2$$

where G = acceleration due to gravity

The integrator transfer function is given by

$$I(s) = \frac{s}{(s/3 + 1)^2}$$

Note the integrator low-frequency roll-off of 3 rad/sec to avoid the application of an infinite d.c. gain to any steady-state components in the accelerometer signal.

According to the inner-loop block diagram shown in Fig. 4, the closed loop transfer function from g_D to g for $\gamma = 8$, $\Omega = 31.4$ rad/sec, $\omega_g/\Omega = 3$, and $K = 3$ is

$$H(s) = 0.58\,\frac{(s/p_1-1)(s/p_1^*-1)(s/p_2-1)(s/p_2^*-1)}{(s/p_1'-1)(s/p_1'^*-1)(s/p_2'-1)(s/p_2'^*-1)}$$

where $p_1 = -300 \pm 300\,j$

$p_2 = -12.2 \pm 93.4\,j$

$p_1' = -305 \pm 471\,j$

$p_2' = -7.0 \pm 93.0\,j$

The corresponding inner-loop root locus is shown in Fig. 5.

Then from the outer-loop block diagram in Fig. 6, the final closed loop transfer function from g_D to g is readily obtained. The corresponding outer-loop locus is shown in Fig. 7.

It is seen that a reduction in bending response to $1/1+K = 0.25$ of the original value, i.e., an attenuation of 75%, at any reasonable bending damping ratio, and without significant change in bending natural frequency, can thus be obtained. The control system achieves the desired attenuation of flatwise bending response, and associated vertical inertial vibratory shear, postulated in the section Technical Discussion.

Note that a similar system can be used to control blade flapping response to either low- or high-frequency airloads. An early example is described in the Appendix and in Ref. 3.

Also note that the same modal control approach can be applied to blade in-plane or torsional motion; application to damping augmentation is described in the Appendix and in Refs. 4 and 5.

Model Design and Construction

The rotor test facility is shown in Fig. 8. For simplicity and ease of modification it was decided to equip a single rotor blade with electro-mechanical pitch control, counter balanced by two "dummy" blades of 5/8 inch steel drill rod and adjustable counterweights. Geometric restrictions were imposed upon the hardware, however, to make it possible to add two more identical but separate pitch actuators without redesign.

The blade used in the test rotor was the same as that of Reference 3, having a NACA 0012 section with a 21.2-inch length and two-inch chord. It had an eight degree linearly decreasing twist from root to tip and was constructed of fiberglass with aluminum reinforcing. The blade was connected to thr rotor hub by means of a ball-and-socket root fixture permitting flapping, lagging and feathering degrees of freedom about the same point. A complete set of rotor parameters can be found in Ref. 3.

The individual-blade-control assembly consisted of a shaft-mounted servo motor that, through a series of linkages, acted as a position controller of the rotor blade pitch angle. The motor/tachometer was mounted between two 1/4-inch-thick disks of aluminum, which also held two counterweights to offset the inertia contribution of the motor. These disks were fixed to the shaft by two aluminum blocks containing two setscrews and a keyway. Also, attached to the forward disk was an aluminum support for the transmission shaft of the control assembly.

This transmission shaft was mounted at a right angle to the motor shaft, and was given its rotation by a spiral-beval gear that was driven by a pinion on the motor shaft, with a 2:1 gear reduction ratio. This same shaft was attached to a thin aluminum bar that had a threaded rod inserted through its other end, and parallel to the transmission shaft. Mounted on the threaded rod was yet another actuator link that consisted of two rod ends screwed together by a threaded metal coupling. The other end of the link was connected to a bolt that passes through the blade pitch axis.

The rotor blade was rigidly attached to a steel fork assembly that, in turn, bolted to the inner race of a spherical bearing. The spherical bearing was then contained within a steel support block that was clamped fast to the main rotor hub; thus allowing fully articulated blade motion with concentric pitch, flap and lead-lag axes, offset from the hub by approximately two inches. The blade root fixture was instrumented with strain gauges mounted on a .005-inch-thick curved steel flexure that was free to turn about the lead-lag

axis, but gave a torsional output corresponding to blade flapping, and a bending output corresponding to blade pitch angle. This particular flexure geometry was chosen as a solution to the problem of uncoupling the three rigid degrees of freedom of the blade for purposes of measurement. A thickness of .005 inches was selected for the flexure to produce a significant signal for small blade deflections, while at the same time providing negligible resistance to the blade flapping motion.

Since the servo motor was to function as a position control device, it was necessary to incorporate appropriately weighted feedback signals to the motor amplifier. These signals were the motor speed, taken from the tachometer, and the angular position, measured from the torsional stain gage mounted on the steel fixture attached to the blade.

Test results for the IBC vertical vibration system will be presented in the near future; test results for related systems are described in the Appendix.

Conclusions

From the preceding theoretical considerations and results the following conclusions can be drawn:

(1) The concept of reducing blade first mode elastic bending and the resulting vertical vibration by feedback control of the effective modal inertia, damping, and stiffness is shown to be feasible.

(2) All necessary information to effect (1) can be obtained from three flatwise-oriented accelerometers, each at a different spanwise location.

(3) Rotor blade flapping, inplane, and/or torsional motion can be reduced by feedback control of the effective inertia, damping, and stiffness of the appropriate modes in a manner similar to that of the present application.

Acknowledgement

This paper is based on the work of not only the author but also of staff members and past and present students of the MIT VTOL Technology Laboratory. Chief contributors were R.M. McKillip Jr. and P.H. Bauer; other important contributions were made by B.L. Behal, C.R. Cole, and T.R. Quackenbush.

References

1. Kretz, M., "Research in Multicyclic and Active Control of Rotary Wings", Vertica, 1, 2, 1976.

2. Ham, N.D., "A Simple System for Helicopter Individual-Blade-Control Using Modal Decomposition", Vertica, 4, 1, 1980.

3. Ham, N.D. and McKillip, R.M. Jr., "A Simple System for Helicopter Individual-Blade-Control and Its Application to Gust Alleviation", Proc. Thirty-Sixth AHS Annual National Forum, May 1980.

4. Ham, N.D. and Quackenbush, T.R., "A Simple System for Helicopter Individual-Blade-Control and Its Application to Stall-Induced Vibration Alleviation", Proc. AHS National Specialists' Meeting on Helicopter Vibration, Hartford, Connecticut, November 1981.

5. Ham, N.D., Behal, Brigitte L. and McKillip, R.M. Jr., "A Simple System for Helicopter Individual-Blade-Control and Its Application to Lag Damping Augmentation", Vertica, 7, 4, 1983.

6. Guinn, K.F., "Individual Blade Control Independent of a Swash Plate", JAHS, 27, 3, July 1982.

7. Miller, R.H. and Ellis, C.W., "Helicopter Blade Vibration and Flutter", JAHS, 1, 3, July 1956.

8. Shaw, J. Jr., "Higher Harmonic Blade Pitch Control for Helicopter Vibration Reduction: A Feasibility Study", MIT ASRL TR 150-1, December 1968.

9. Wilby, P.G., et al., "An Investigation of the Influence of Fuselage Flow Field on Rotor Loads and the Effect of Vehicle Configuration", Vertica, 3, 2, 1979.

10. Ham, N.D., "Helicopter Blade Flutter", AGARD Report No. 607, January 1973.

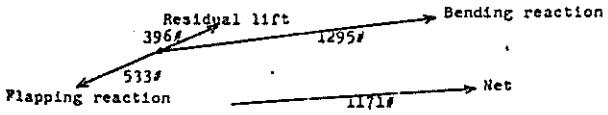

FIG. 1 Net Third Harmonic Vertical Hub Shear and Its Components

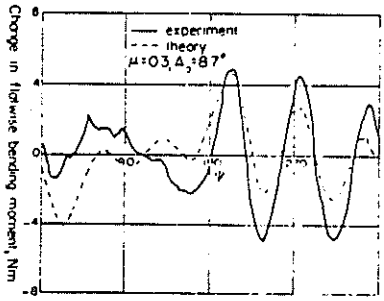

FIG. 2 Predicted and Measured Effect of Fuselage on Model Blade Flatwise Bending Moment

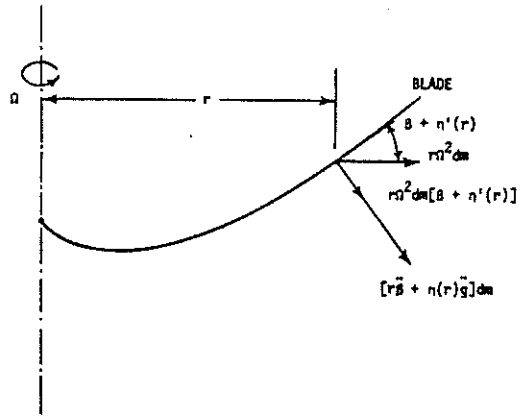

FIG. 3 Blade Flatwise Inertia Forces

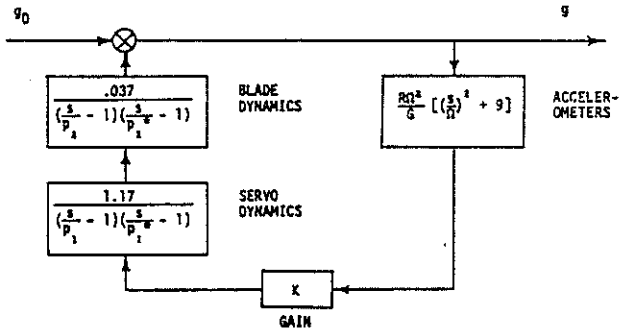

FIG. 4 Inner Loop Block Diagram Yielding H(s) (Vibration System)

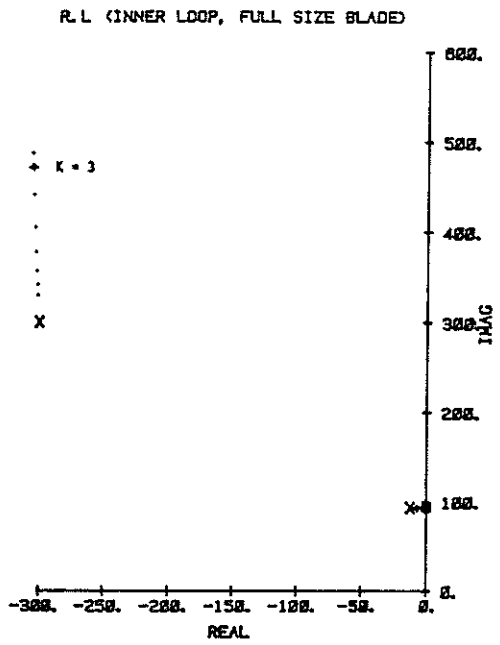

FIG. 5 Inner Loop Root Locus (Vibration System)

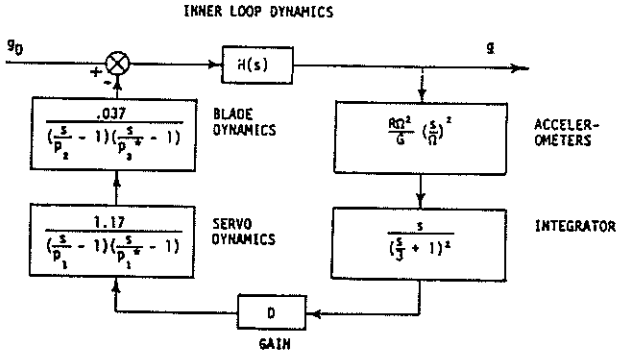

FIG. 6 Outer Loop Block Diagram (Vibration System)

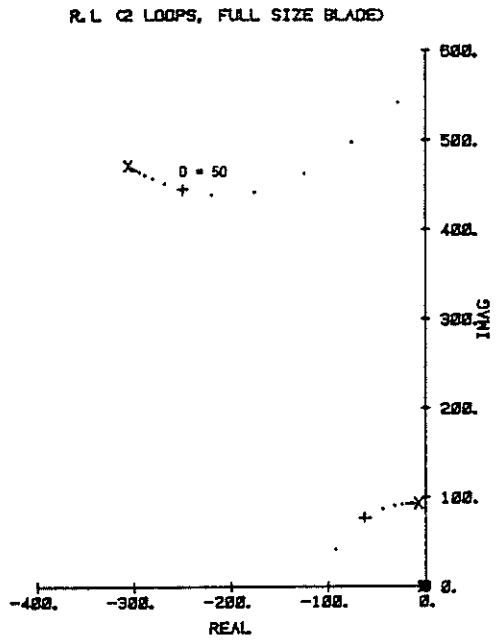

FIG. 7 Outer Loop Root Locus (Vibration System)

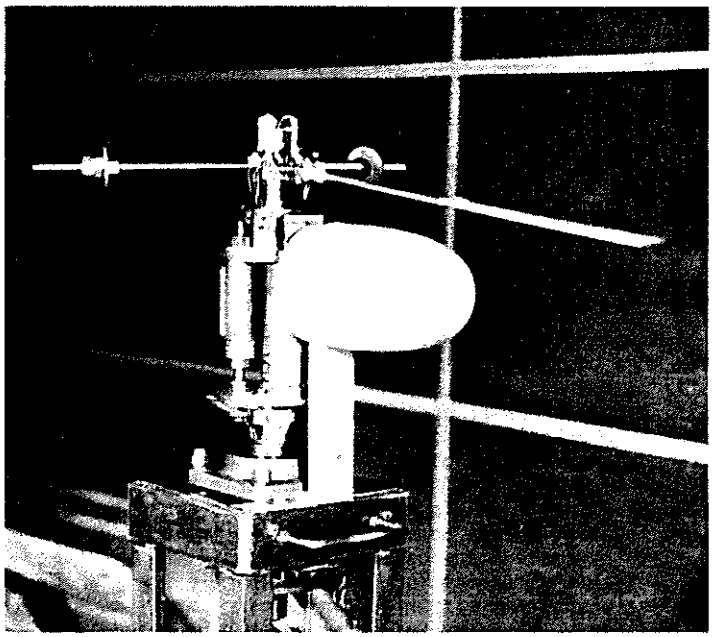

FIG. 8 Individual-Blade-Control Model Rotor Assembly

APPENDIX

Applications of Helicopter Individual-Blade-Control (IBC)

A.1 Gust Alleviation

The Wright Brothers Wind Tunnel at M.I.T. was used for IBC rotor gust alleviation testing. The test section is a 7 ft. x 10 ft. oval, and for rotor testing the turntable is equipped with two trunnions for horizontal mounting of the rotor shaft. This particular orientation was chosen to permit use of the existing sinusoidal gust generator.

In the wind tunnel test, the parameters varied were gust excitation frequency, tunnel speed, and feedback. A typical time history of the gust, flapping, pitch, and accelerometer signals for the $\mu = 0.4$ case can be seen in Figure A.1, and the spectral decomposition of this run is shown in Figure A.2. The information from the spectral analyses of the gust signal was then used as input to produce the solid theoretical curves of Figure A.3. Several Fast Fourier Transform analyses were performed over different segments of data for the open loop cases of the test, and the standard deviation for these data was used to construct the error bars about the data points.

The data for the various cases tested appears to match the theory reasonably well, and the correlation appears to improve with increasing advance ratio. The explanation for this trend may well be the reduction in dynamic inflow effects due to an increase in total rotor inflow.

Figure A.4 shows the effect of increasing open-loop static sensitivity upon the IBC gust alleviation system performance.

Further details are given in Ref. A.1. This reference shows that eighty percent alleviation of gusts or other low frequency disturbances is feasible.

A.2 Stall Flutter Suppression

Reference A.1 showed that appropriate feedback to a position control servo governing blade pitch motion could reduce undesirable blade motions due to low-frequency gust inputs. Similar methods were applied to alleviate the violent torsional motions associated with stall flutter. At high blade angles of attack and certain reduced frequencies, aerodynamic moment hysteresis causes a net input of energy to blade torsional motion, so that any small blade oscillation grows with time. Such a situation is typical of simple oscillating systems with negative damping; stall flutter can be conceived of as a phenomenon caused by a once-per-revolution variation in the effective damping of the blade in pitch. On the advancing side, the blade experiences strong positive damping at low angles of attack, but on the retreating side the effective damping can temporarily become negative, leading to the oscillations described above.

An effective stall flutter suppression system, then, would eliminate this one-per-rev excursion into negative damping. One way to achieve this end is to provide pitch-rate feedback from the blade to the pitch control servo. The details of this concept, its implementation, and the results of experiments utilizing it are given in Ref. A.2.

Typical test results are shown in Figs. A.5 and A.6 for an advance ratio of 0.33. Note that the stall flutter component at 5/rev. is effectively suppressed with increasing feedback.

A.3 Lag Damping Augmentation

To achieve lag damping augmentation, a servomotor controls the pitch angle of the blade whose lag acceleration is sensed by two accelerometers, and an integrator yields the lag velocity which is fed back through a compensator to the blade pitch control. A blade flapping velocity is thus generated which in the presence of blade coning angle, results in an in-plane moment due to Coriolis forces which opposes lag motion and is proportional to lag velocity.

A series of wind tunnel tests was run utilizing white noise excitation of blade pitch. The results are shown in Figs. A.7 and A.8, in terms of lag acceleration magnitude and phase as a function of pitch excitation frequency for the rotor in hover and at advance ratio 0.27. (For details, see Ref. A.3 .)

The amplitude responses in Figs. A.7 and A.8 are inconclusive in demonstrating an increase in lag damping due to the control system. However, the associated phase angle data are conclusive. Both figures show a rotation of the slope of the phase angle versus frequency curve at lag resonance, in the direction of increased lag damping, as K_R is increased. The effect is more pronounced at advance ratio of 0.27 than at hover, possibly reflecting the reduction of adverse dynamic inflow effects with advance ratio. The increase in lag damping ratio due to the control system was determined to be 0.18 in hover and 0.37 at advance ratio 0.27. These values are incremental to the open loop value of 0.37 due to bearing friction.

A.4 Vertical Vibration Alleviation

See Ref. A.4 (main text of this paper).

A.5 Inplane Vibration Alleviation

The blade inplane modes can be controlled using methods similar to those described in Refs. A.3 and A.4. Details will be given in a subsequent report.

A.6 Flapping Stabilization at High Advance Ratio

The individual blade flap damping and restoring force can be augmented using IBC techniques similar to those described in Refs. A.1 and A.4. Details will be given in a subsequent report.

A.7 Stall Alleviation

Blade stall on the retreating side of the disk can be alleviated by activating the IBC system to reduce blade pitch at stall onset. It is hoped to utilize stall-induced lag accelerometer signals above a specified threshold value to trigger the desired IBC action. If accelerometer signals are inadequate in this application, blade pressure signals can be utilized as described in Ref. A.5.

Details will be given in a subsequent report.

A.8 Flying Qualities Enhancement

Blade flapping due to low frequency vehicle pitching, rolling, horizontal and vertical disturbances can be alleviated by the IBC system used for gust alleviation described in Ref. A.1. Since primary helicopter control is achieved through orientation of the rotor thrust vector with respect to the fuselage, tighter control over orientation of the tip path plane (and hence the thrust vector) will improve the vehicle's handling qualities.

A.9 Performance Enhancement

Preliminary work has indicated that there are substantial performance increments to be obtained from the introduction of appropriate higher harmonic control to the helicopter rotor. Since individual blade control is a generalization of higher harmonic control, similar benefits can be expected in this application.

A.10 Automatic Blade Tracking

Blade aerodynamic or mass mismatch due to battle (or other damage) or faulty rigging procedures leads to rotor out-of-track and high 1P vibration. This condition can be alleviated by minimizing the difference between individual blade flatwise accelerometer signals using the Individual-Blade-Control system.

Appendix References

A.1 Ham, N.D. and McKillip, R.M. Jr., "A Simple System for Helicopter Individual-Blade-Control and Its Application to Gust Alleviation", Proc. Thirty-Sixth AHS Annual National Forum, May 1980.

A.2 Ham, N.D. and Quackenbush, T.R., A Simple System for Helicopter Individual-Blade-Control and Its Application to Stall-Induced Vibration Alleviation", Proc. AHS National Specialists' Meeting on Helicopter Vibration, Hartford, Connecticut, November 1981.

A.3 Ham, N.D., Behal, Brigitte L. and McKillip, R.M. Jr., "A Simple System for Helicopter Individual-Blade-Control and Its Application to Lag Damping Augmentation", Vertica, 7, 4, 1983.

A.4 Ham, N.D., "Helicopter-Individual-Blade-Control and Its Applications", Proc. Thirty-Ninth AHS Annual National Forum, May 1983.

A.5 Kretz, M., "Active Elimination of Stall Conditions", Proc. Thirty-Seventh AHS Annual National Forum, May 1981.

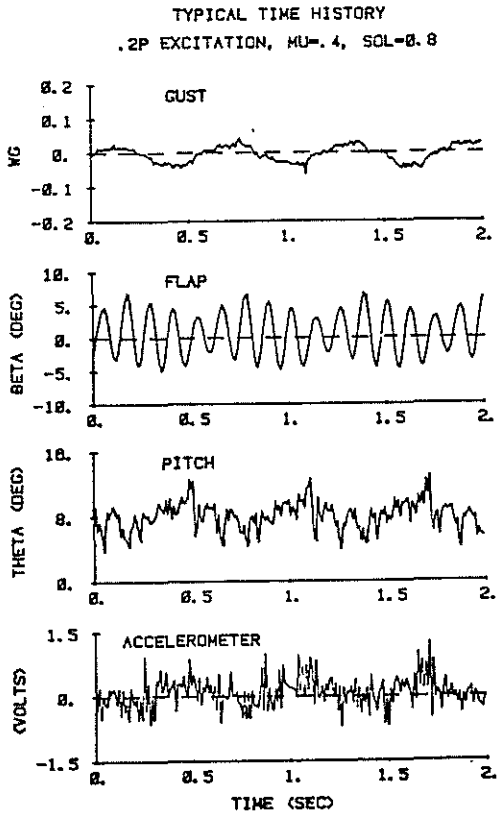

FIG. A.1 Typical I.B.C. Gust System Experimental Time History

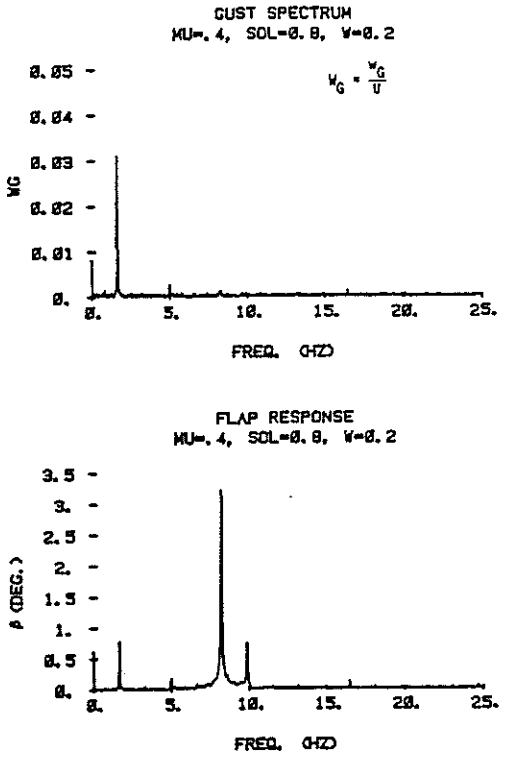

FIG. A.2 Spectral Decomposition of Experimental Gust and Flap Angle Data

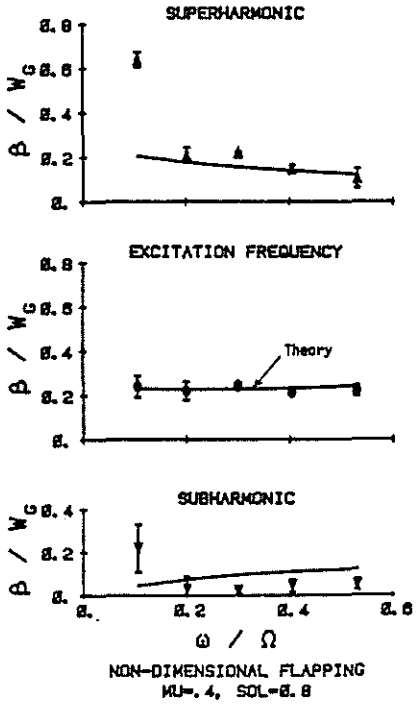

FIG. A.3 Non-Dimensional Flap Angle Response to Gust

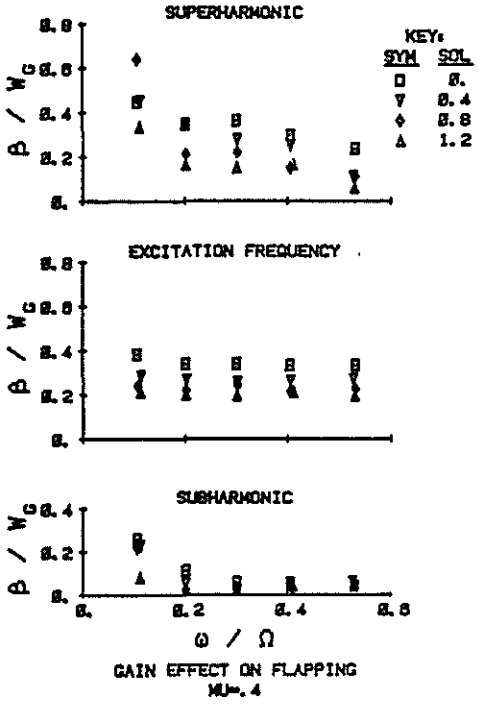

FIG. A.4 Effect of Feedback Gain on Flap Angle Response to Gust

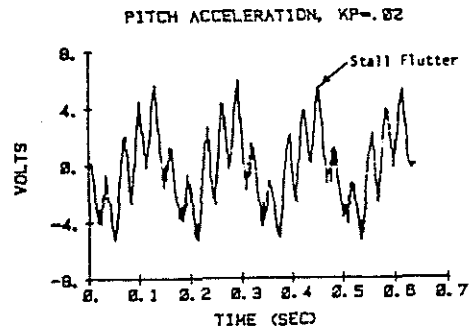

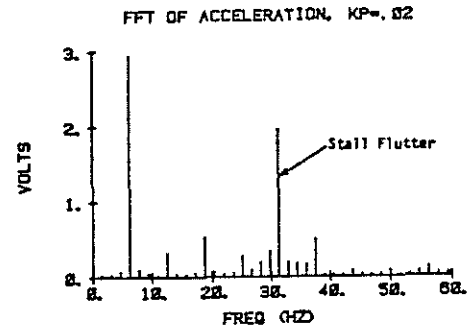

FIG. A.5 Low Feedback Stall Flutter Test, Ω = 6.1 Hz, μ = 0.33

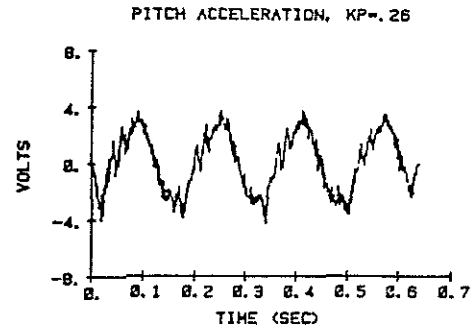

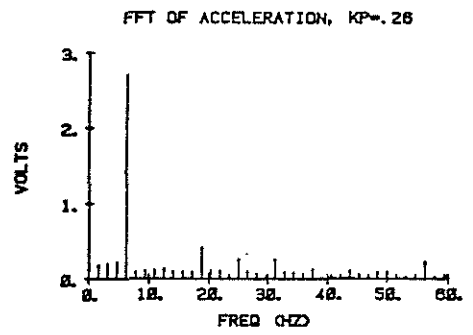

FIG. A.6 High Feedback Stall Flutter Test, Ω = 6.1 Hz, μ = 0.33

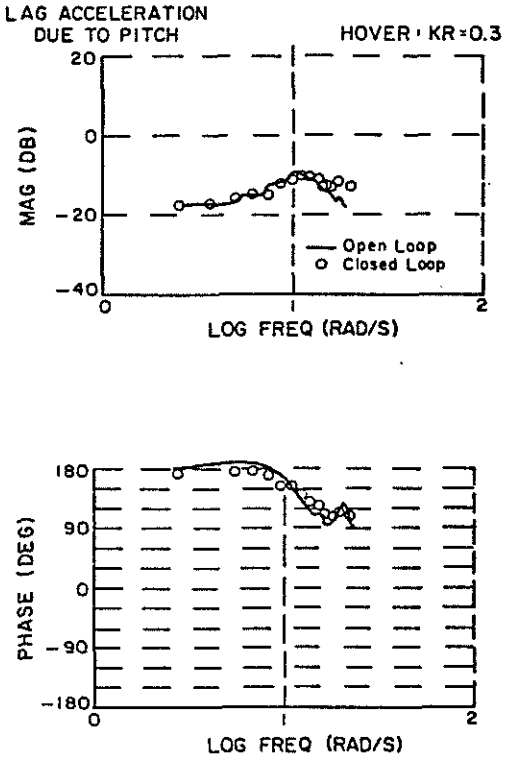

FIG. A.7 Experimental Results, μ=0, Ω=37.7 rad/s. Pitch θ to Lag Accelerometer Difference Signal 1/2 (R-e)ℓ

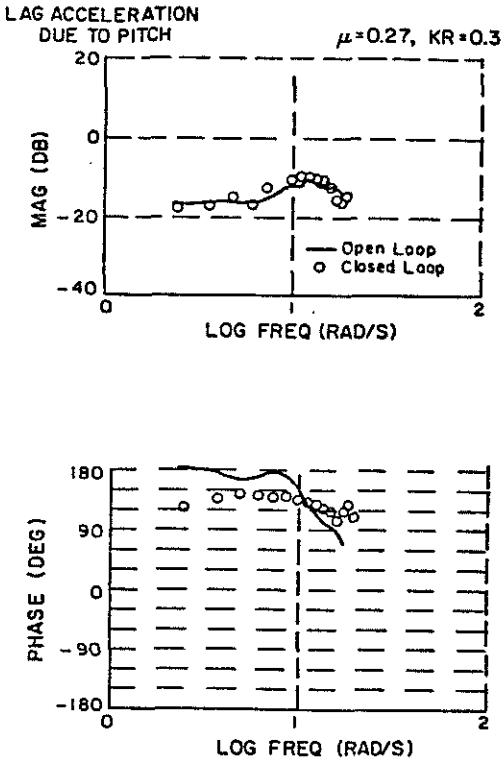

FIG. A.8 Experimental Results, μ=0.27, Ω=37.7 rad/s. Pitch θ to Lag Accelerometer Difference Signal 1/2 (R-e)ℓ